

Mechanism of Iminium Salt-Catalyzed C(sp3)-H Amination: Factors Controlling Hydride Transfer versus H-Atom Abstraction

Madeline E. Rotella, ^{†©} Robert M. B. Dyer, [‡] Michael K. Hilinski, *, ^{‡©} and Osvaldo Gutierrez*, ^{†©}

Department of Chemistry and Biochemistry, University of Maryland, College Park, Maryland 20742-4454, United States

Supporting Information

ABSTRACT: Carbon-nitrogen bonds are extremely prevalent in pharmaceuticals, natural products, and other biologically relevant molecules such as nucleic acids and proteins. Intermolecular amination of C(sp³)-H bonds by catalytic nitrene transfer is a promising method for forging C-N bonds. An organocatalytic approach to nitrene transfer by way of an iminium salt offers a site-selective method for C(sp³)-H amination. Understanding of this amination mechanism including the nature of the relevant intermediates and the factors controlling the mechanism of the N-H bond formation step would aid in the design of catalysts and $C(sp^3)$ -H amination methods. In this work, the mechanism of the iminium salt-catalyzed $C(sp^3)$ -H amination via nitrene transfer was elucidated computationally using quantum mechanical methods and molecular dynamics simulations. Dispersion-corrected density functional theory calculations provide support for an open singlet biradical species in equilibrium with the lower energy triplet species. Calculations further reveal that, while the singlet biradical species undergoes N-H bond formation by a hydride transfer process, the triplet species forms the N-H bond by H-atom abstraction. Molecular dynamics simulations rule out the possibility of a fast rebound of the carbon substrate following N-H bond formation. A predictive model for mode of activation and site selectivity that is consistent with experimental observations is presented.

KEYWORDS: catalysis, dynamics, organocatalysis, amination, C-H activation, biradicals

1. INTRODUCTION

The prevalence of nitrogen in FDA-approved drugs, natural products, and molecules central to life (e.g., nucleic acids and proteins) has elevated the development of methods for the formation of C-N bonds to a place of prominence in modern synthetic methods research.^{1,2} In particular, intermolecular amination of C(sp³)-H bonds via catalytic nitrene transfer holds great promise for streamlining synthesis, and applications such as the late-stage functionalization of bioactive compounds have captured widespread interest.3,4 However, modulation of site- and stereoselectivity in these reactions via catalyst control is still a fundamental challenge.

The discovery of different modes of catalytic nitrene transfer that are distinct from existing transition metal-catalyzed methods holds promise for hastening the development of reactions exhibiting complementary selectivity. 6 Recently, the Hilinski laboratory disclosed the first example of organocatalytic nitrene transfer and demonstrated the method's capability in the context of site-selective $C(sp^3)$ -H amination (Scheme 1) and aziridination.8 The catalyst, an iminium salt, is proposed to react with an iminoiodinane nitrene precursor to produce a diaziridinium salt⁹ as the active oxidant, which then reacts with the substrate to produce the observed product and

Scheme 1. Iminium Salt-Catalyzed C-H Amination

Representative products:

regenerate the catalyst (Scheme 1). Conceptually, this extends organocatalytic atom-transfer oxidation reactions, which are well established for oxygen transfer via dioxirane and oxaziridinium intermediates, to nitrene transfer. More broadly,

Received: August 22, 2019 Revised: December 6, 2019 Published: December 9, 2019

^{*}Department of Chemistry, University of Virginia, Charlottesville, Virginia 22904-4319, United States

it confirms the possibility of developing sustainable strategies for atom-transfer C–H amination that are outside of the current transition metal paradigm.

Initial investigations into the scope of iminium-catalyzed C-H amination revealed its ability to oxidize weak $C(sp^3)$ -H bonds such as benzylic C-H bonds, α -positions of ethers and protected amines, and highly activated aliphatic substrates (Scheme 1). Accompanying the report of the catalytic method and its scope, preliminary mechanistic investigations supported the initial hypothesis; namely, that the reaction of the iminoiodinane with the iminium catalyst produces an intermediate that reacts as though it were a nitrenoid species. Preliminary experiments revealed a dependence of amination yield on iminium salt structure and a limited role of the tetrafluoroborate counterion in promoting the observed reactivity, supporting the hypothesis of iminium ion involvement in the formation of an organic nitrenoid equivalent. This initial conclusion is further corroborated by new control experiments using tetrabutylammonium tetrafluoroborate as an organic-soluble source of the counterion (Scheme 2). No

Scheme 2. Control Experiments Confirming a Key Role for the Iminium

reaction was observed either in the absence of a catalyst or with catalytic amounts of *n*-Bu₄NBF₄. In addition to providing additional evidence of a limited role for tetrafluoroborate in initiating nitrenoid transfer from iminoiodinanes, this experiment also indicates that the iminium salt is not simply acting as a phase-transfer catalyst.

Despite these initial investigations, substantial unanswered mechanistic questions remain, such as the potential existence and fate of the proposed diaziridinium intermediate. For example, diaziridinium intermediate 1a could undergo N-N homolysis to form 1b or heterolysis to form 1c (Scheme 2). Further, 1b and 1c could interchange via an intramolecular single electron transfer (SET) and can undergo intersystem spin crossing to form singlet or triplet species. Moreover, contrary to the rich mechanistic literature of oxyfunctionalization of $C(sp^3)$ -H bonds (i.e., dioxirane and Fe-oxo chemistry), there is almost no knowledge about the mechanisms of azafunctionalization of $C(sp^3)$ -H bonds. ¹⁰ In order to broaden substrate scope and to address current challenges in C-H functionalization, it will be critical to develop a detailed understanding of the mechanism and to apply that understanding to the design of catalysts and methods. Herein, we turn to quantum mechanical calculations and quasi-classical direct-dynamics simulations to understand the nature of the active species, elucidate the mechanism for C-H activation, and gain insights into the origin of C-H site selectivity. Overall, a refined mechanistic proposal that is consistent with experimental observation and a predictive model for mode of activation and site selectivity is presented.

2. RESULTS AND DISCUSSION

From preliminary experimental observations and proposed mechanisms for C-H activation via dioxiranes, we initially envisioned three potential pathways for C-H activation from diaziridinium 1 (Scheme 3). For simplicity, the counterion is omitted (See Figure S1 in the Supporting Information for an explanation of the counterion omission). The concerted nitrenoid nitrogen insertion (PATH A), in analogy to the concerted "oxenoid" mechanism proposed by Murray et al. and Curci et al. for dioxirane C-H oxidation, 11 could directly form the C-N bond and regenerate the iminium catalyst. 12 Gassman demonstrated that singlet nitreniums could undergo spin inversion to form the triplet nitrenium ions and singlettriplet gaps are sensitive to substituent patterns. 13 Through photolysis, Falvey et al. demonstrated spin-selective reactivity of the parent nitrenium (NH₂⁺). Specifically, singlet NH₂⁺ undergoes hydride transfer from toluene while triplet nitrenium undergoes H-atom abstraction (HAT). These results demonstrate that singlet nitreniums undergo 2 electron nucleophilic attack while the triplet nitreniums react via radical chemistry. Based on this precedent, we propose two alternative mechanisms, namely PATH B and PATH C. In PATH B, compound 1 (e.g., open-form singlet or triplet biradical 1b) could promote H-atom abstraction, leading to the alkyl radical int-1 complex. In turn, akin to the Fe-oxo C-H oxidation mechanism, the -NHR group can then "rebound" to the alkyl radical to form the amination product 2. In PATH C, 1 can instead promote C-H activation via a "hydride transfer mechanism" akin to those observed for singlet nitreniums, leading to the carbocation int-2 complex. In turn, NHR displacement followed by nucleophilic attack on the carbocation will lead to 2.

2.1. Reaction of Iminium Salts with Amination Reagent Leads to Distinct Diaziridinium and Amidyl Biradical Intermediates. Our mechanistic analysis is broken down into five parts based on our computational findings: (1) mechanistic proposal leading to the production of four distinct amidyl-iminium and diazaridinium intermediates, (2) analysis of the nature of these intermediates, (3) mechanistic proposal for C–H activation from the lowest energy of these intermediates, (4) effect of carbon substrate on the mechanism

Scheme 3. Possible Mechanisms for Iminium Salt-Catalyzed Aliphatic C—H Amination

of C–H activation, and (5) molecular dynamics simulations to investigate the time scale for C–H activation and approximate lifetime of the purported intermediates.

We began our mechanistic studies by constructing the potential energy surface using the UB3LYP-D3/6-311+G(d,p)-SDD(I)-CPCM(DCM)//UM06-2X/6-31+G(d,p)-LANL2DZ(I)-CPCM(dichloromethane) level of theory (see the Supporting Information for computational methods and Figures S2-S4 for a discussion of the method choice). We chose DFT methods for our computational analysis because DFT methods, and in particular the UM06-2X functional, correctly predict experimental trends for open-shell species with low computational cost compared with multireference methods (e.g., CASPT2). As shown in Figure 1, the iminium organocatalyst can adopt a downward (A) or an upward (A') puckered 5-membered ring conformation. Since these two conformations are nearly isoenergetic, we initiated our computational studies from these two conformations. As shown in Figure S5, the iminium ion organocatalyst A can undergo nucleophilic attack by the iminoiodinane MeI=NMs via TS_{A-B} (barrier of 19.7 kcal/mol) to form adduct B, uphill by 17.3 kcal/mol. In turn, complex B can then undergo 3membered ring closure via TS_{B-E} (overall barrier of 26.1 kcal)

with concomitant release of the iodomethane to form the "closed-form" diaziridinium E intermediate (see Figure S6 in the Supporting Information), overall 3.3 kcal/mol downhill in energy. This (singlet) intermediate E could promote $C(sp^3)$ H activation by engaging with the alkane substrate (vide infra) or can first undergo a homolytic ring opening via the singlet spin state to form open intermediate D via TS_{E-D} (barrier of only 13.8 kcal/mol) and then promote C(sp³)-H activation (vide infra). Notably, in contrast to the closed-formed amidyliminium species E (the singlet-triplet gap is >60 kcal/mol), the singlet and triplet "open-form" biradical species D are isoenergetic. Thus, we considered both singlet and triplet "open-form" D intermediates and only the singlet spin state of E for C-H activation (vide infra). A heterolytic cleavage transition state, located using restricted DFT, leading to the closed-shell nitrenium intermediates is found to be much higher in energy (23.0 kcal/mol; see Figure S7 in the Supporting Information) and was not considered further.

Alternatively, A could undergo a conformational change to form A' (not calculated) followed by nucleophilic attack by MeI=NMs via the lower energy TS_{A'-C'} (Figure 1; barrier of 12.2 kcal/mol compared to barrier of 19.7 kcal/mol for TS_{A-B}) to form adduct C'. Presumably, TSA-B is higher in energy due to the negative steric interactions between the neighboring axial groups, which are not present in $TS_{A'-C'}$ (See Figure S8 in the Supporting Information). Intermediate C' can then undergo a concerted ring closure with simultaneous removal of the iodomethane via $TS_{D''-E''}$ (barrier is 16.8 kcal/mol) to give the diaziridinium E'. Notably, calculations favor the stepwise process in which the MeI dissociation occurs first (via $TS_{C'-D'}$) to form an amidyl-iminium intermediate D', which can quickly undergo ring-closing (via $TS_{D'-E'}$) leading to E' $(TS_{D''-E''}$ versus $TS_{D'-E'}$). Further, we also found a conformational change transition state (TS_{B-C'}) with a low energy barrier that connects "down" and "up" I(II) intermediates, B and C', respectively, as well as two other conformational change transition states (TS_{D-D'} and TS_{E-E'}), which connect the down D and E intermediates and the up D' and E'intermediates. Given that singlet and triplet "open" amidyliminium intermediates (D and D') are nearly isoenergetic, in principle, C-H activation could occur from the singlet or triplet spin states. Thus, we considered single and triplet open-(amidyl-iminium) and closed-form (diaziridinium) intermediates (D, D', E, and E') as potential species for C-H activation.

2.2. Nature of Open- (Amidyl-Iminium) and Closed-Form (Diaziridinium) Intermediates. To better understand the mechanism of C-H activation, we investigated the electronic nature of the open- and closed-form intermediates. The singlet and triplet forms of both geometries were located (Figure 1). As shown in Scheme 4, the singlet-triplet gap of these amidyl-iminium intermediates is small (<2 kcal/mol). Further, closer inspection of the open-form amidyl-iminium intermediates revealed that the singlet nitrenium D and D' can be classified as biradical amidyl-iminium species (i.e., 1b in Scheme 3) as noted by the Mulliken spins at both nitrogen atoms of close to ± 1.17 The open triplet nitrenium intermediates ^tD and ^tD' are also biradicals resembling 1b (Scheme 3) with Mulliken spins on the nitrogen atoms of close to +1. As shown by Gassman, the singlet open nitrenium species could undergo spin inversion to produce the lowerenergy triplet species, which can promote a distinct mode of C-H activation (vide infra). On the other hand, the energy difference between the diaziridinium singlet and triplet spin

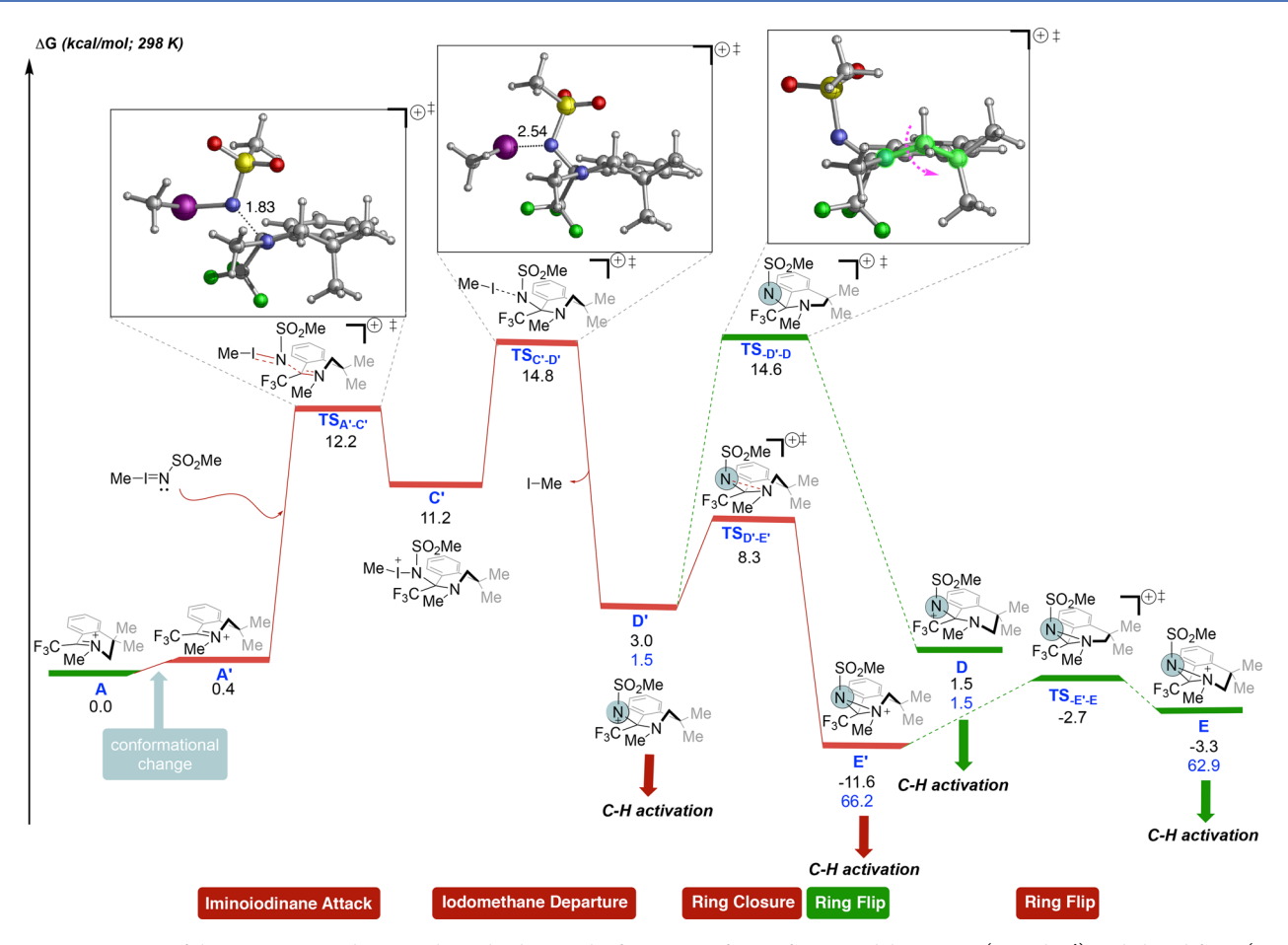
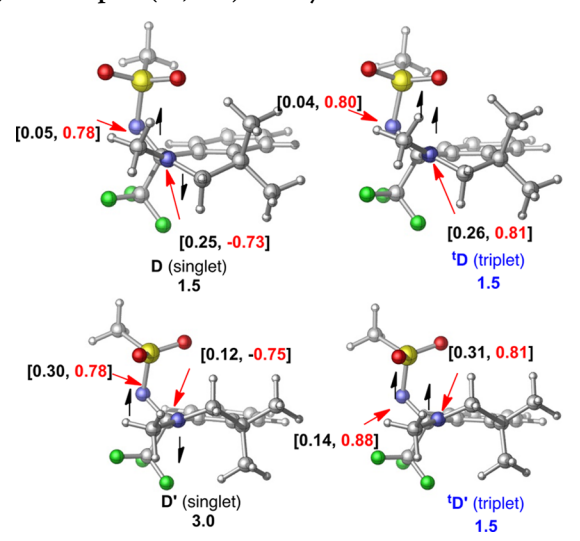


Figure 1. Energetics of the reaction coordinate pathway leading to the formation of open-form amidyl-iminium (\mathbf{D} and \mathbf{D}') and closed-form (\mathbf{E} and \mathbf{E}') diaziridinium intermediates. Free energies (kcal/mol) are computed at the UB3LYP-D3/6-311+G(d,p)-SDD(I)-CPCM(DCM)//UM06-2X/6-31+G(d,p)-LANL2DZ(I)-CPCM(dichloromethane) level. Singlet energies are given in black and triplet energies are in blue.

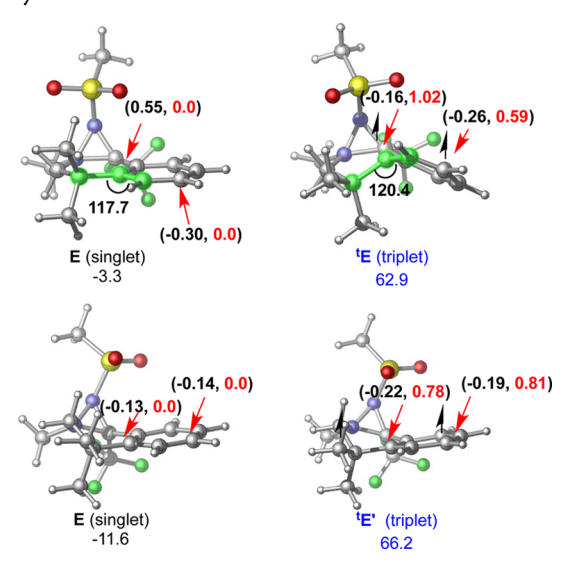
Scheme 4. Closer Inspection of the Open-Form Singlet (D, D') and Triplet (D, D') Amidyl-Iminium Intermediates



"Mulliken charges and spins of the nitrogen atoms are shown in black and red, respectively. Free energies (kcal/mol) are computed at the UB3LYP-D3/6-311+G(d,p)-SDD(I)-CPCM(DCM)//UM06-2X/6-31+G(d,p)-LANL2DZ(I)-CPCM(dichloromethane) level of theory.

states (Scheme 5) was significantly higher in energy (>65 kcal/mol); thus, the triplet spin states from 'E and 'E' were not

Scheme 5. Comparison between the singlet and triplet states of the diaziridinium intermediates E, E' and $^{\rm t}$ E, $^{\rm t}$ E'. Relevant Mulliken charges and spins are given in black and red, respectively, and relevant bond angles are in black. Free energies (kcal/mol) are computed at the UB3LYP-D3/6-311+G(d,p)-SDD(I)-CPCM(DCM)//UM06-2X/6-31+G(d,p)-LANL2DZ(I)-CPCM(dichloromethane) level of theory



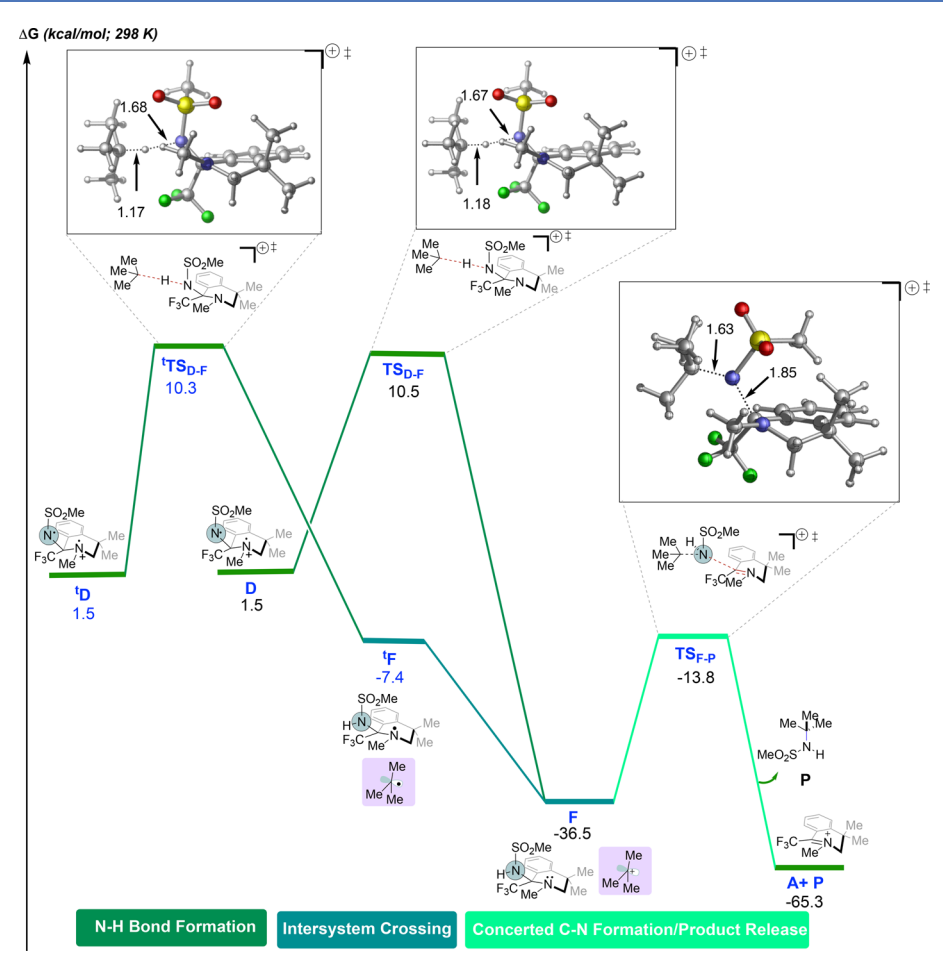


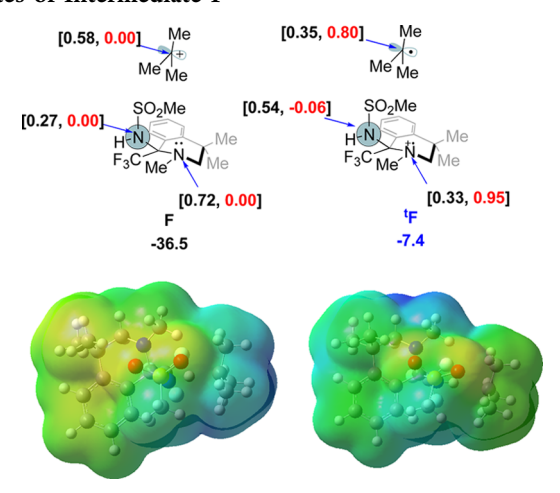
Figure 2. Lowest-energy pathways leading to C–H activation via open diaminium species D, which undergoes N–H bond formation to give F. Free energies (kcal/mol) are computed at the UB3LYP-D3/6-311+G(d,p)-SDD(I)-CPCM(DCM)//UM06-2X/6-31+G(d,p)-LANL2DZ(I)-CPCM(dichloromethane) level of theory. Singlet energies are given in black, and triplet energies are in blue.

considered further. We attribute this large energy gap to disruption of aromaticity as evidenced by the localization of the electron spin in the aryl ring. For example, the free radical in the triplet form ^tE is located at the phenyl carbon (indicated by Mulliken spin of 1.02; red). Overall, these results suggest that the closed-form diaziridinium E and E' exist only in the singlet state, which are significantly lower in energy than the triplet closed-form species. On the contrary, the singlet state (amidyl-iminium) of the open form is in equilibrium with the triplet biradical state. Electrostatic potential maps also support the nature of the intermediates as described above (See Figures S9 and S10 in the Supporting Information).

2.3. Mechanism for C-H Activation by Diaminium and Amidyl-Iminium Intermediates. Having investigated the nature of the open and closed intermediates, we then focused on exploring the viable pathways for C-H activation by the amidyl-iminium and diaziridinium intermediates. For simplicity, we will limit the discussion to the lowest-energy pathway from the open intermediates (Figure 2) since the pathways for C-H activation from the thermodynamically favored closed-formed diaziridinium intermediates E and E' are higher in energy (See Figures S11 and S12 for the full pathway in the Supporting Information for details). Further, we initially started with the tertiary alkyl radical as the substrate although later we also explored the effects of other C-H bonds. We were interested in investigating the possibility of a hydrogen-atom-transfer (HAT) mechanism (homolytic

cleavage) as opposed to a hydride transfer mechanism (heterolytic cleavage) from the putative amidyl-iminium intermediates. Hydride transfer models have been proposed for oxidation reactions catalyzed by oxoammonium salts as well as for intramolecular C-H amination, which led us to hypothesize that this process was plausible for the nitrenium species. 18 To probe the nature of the C-H activation step, we turned to Mulliken charge and spin analysis. We identified a HAT mechanism if the spin on the resulting carbon is approximately +1 and the overall charge is ~ 0 . Alternatively, a hydride transfer mechanism is identified by the formation a carbocation species (spin ~ 0 and a charge approximately +1). As shown in Figure 2, singlet amidyl-iminium D undergoes C-H activation through a hydride mechanism via TS_{D-F} (barrier of 10.5 kcal/mol), leading to the formation of F, a carbocation as determined by analysis of the spin and charge of the intermediate (Scheme 6). Subsequently, F can undergo concerted N-C bond formation and C-N bond breaking via TS_{F-P} (barrier is 22.7 kcal/mol from F) to give the desired product P and regenerate the iminium ion organocatalyst A. Alternatively, the singlet open nitrenium species D can undergo spin inversion to give the energetically similar triplet species ^tD. This triplet species undergoes HAT via TS_{D-F} to form radical complex F (barrier of 10.3 kcal/mol) as determined by the presence of the radical on the carbon substrate (Scheme 6; see Figure S13 in the Supporting Information for the other conformer F' and tF'). In principle,

Scheme 6. Comparison of Singlet (Left) and Triplet (Right) States of Intermediate F^a



"Mulliken charges and spins for select atoms are given in black and red respectively. Electrostatic potential maps (EPM) are given as well. Free energies (kcal/mol) are computed at the UB3LYP-D3/6-311+G(d,p)-SDD(I)-CPCM(DCM)/UM06-2X/6-31+G(d,p)-LANL2DZ(I)-CPCM(dichloromethane) level of theory.

^tF can undergo radical rebound but the relative barriers for this process were high (34.8 kcal/mol), and quasi-classical dynamic calculations from ^tTS_{D-F} show that 64% of the trajectories led to ^tF and 36% led back to open-form ^tD without any trajectories leading to radical rebound (See Figure S14 in the Supporting Information). Overall, these results support facile intersystem crossing from ^tF to form the carbocation F complex followed by C–N bond formation and subsequent product release.

We also explored the C-H activation pathway from the "up" conformational intermediates D' and tD', (singlet and triplet, respectively). As shown in Figure S12 (red; left), the lowestenergy pathway (from D' or ^tD') proceeds from ^tD' through a HAT mechanism (via ^tTS_{D'-F'} with overall barrier of 12.0 kcal/ mol) to form alkyl radical complex ^tF'. The triplet species ^tF' will then undergo an intersystem crossing to form the lowerenergy singlet carbocation species F' (downhill by 41.6 kcal/ mol). Finally, this intermediate F' will undergo a concerted C-N bond formation and product release via $TS_{F'-P}$ (barrier is only 23.8 kcal/mol from F'). Analysis of the Mulliken spin of the F' and tF' intermediates supports this hypothesis that the triplet ^tD' undergoes HAT (radical process) to produce a radical carbon species while the singlet undergoes hydride transfer (anionic process) to produce a carbocation (Figure S13). Overall, the open-form amidyl-iminium biradical intermediates D and D' are responsible for C-H activation. Moreover, akin to nitrenium chemistry, the mechanism is spincontrolled in which the singlet amidyl-iminium undergoes a "hydride" transfer, leading to a carbocation while the triplet amidyl-iminium biradical undergoes a HAT to form an alkyl radical. In the case of the triplet alkyl radical complexes tF or ^tF', the species then undergoes an intersystem crossing, leading to the singlet alkyl carbocation F or F', respectively. Notably, for the tertiary substrate, both HAT and hydride mechanisms are competitive (within 0.2 kcal/mol).

2.4. Effect of Substrate on the C–H Activation Step: HAT versus Hydride Transfer. Our results show that both singlet and triplet amidyl-iminium biradical intermediates

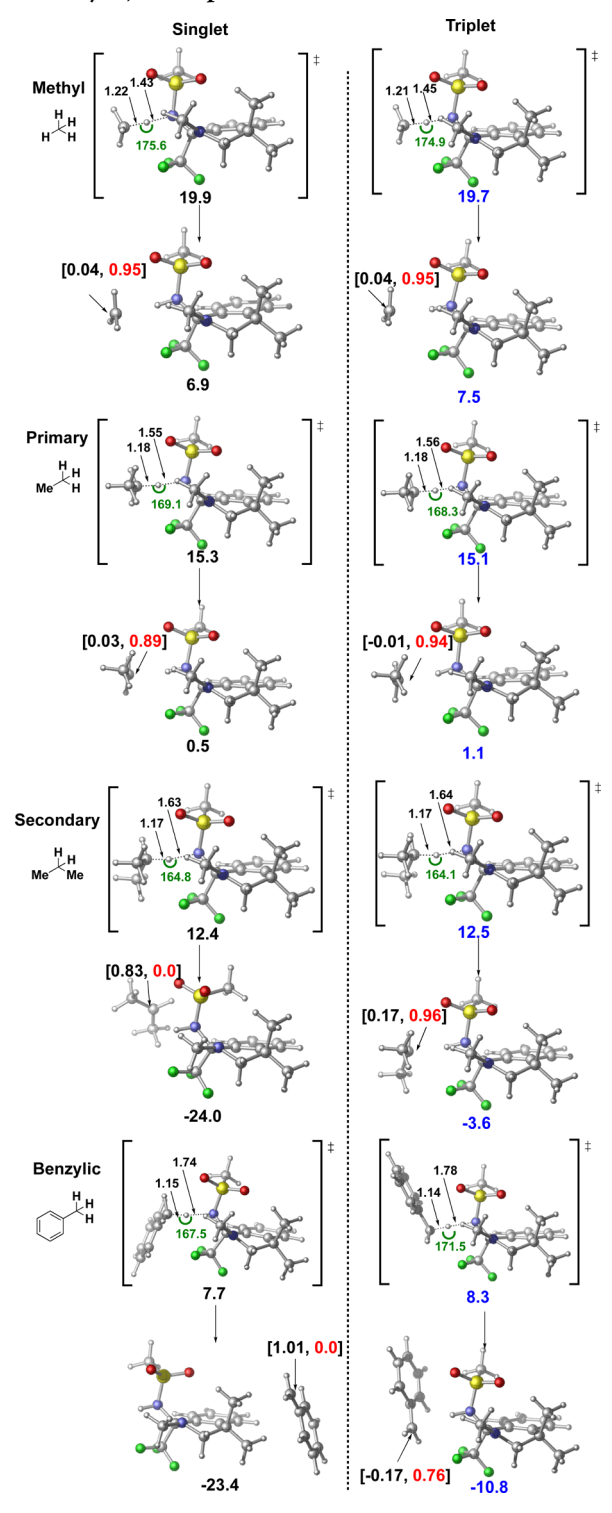
could be responsible for C-H activation. Moreover, for singlet species, the N-H bond formation step proceeds via a nucleophilic "hydride" mechanism, leading to the formation of a carbocation complex (Figure S15). On the other hand, the triplet species proceeds via a HAT mechanism leading to the formation of an alkyl radical, which could then undergo intersystem crossing and single-electron transfer (SET) to form the energetically favored singlet carbocation complex (Figure S16). Intrigued by these results, we explored the effect of the substrate (e.g., methyl vs 1° vs 2° vs 3° vs benzyl) in the C-H activation step (e.g., from singlet and triplet amidyliminium intermediates). For simplicity, we only discuss the C-H activation step from the "down" conformation of the singlet and triplet amidyl-iminium intermediate since the barriers from the "up" conformation were found to be higher in energy (see Figures S17-S20 in the Supporting Information for full details). As shown in Scheme 7, from this analysis we observe that (1) the overall barriers from C-H activation are correlated to the bond dissociation of the alkyl substrate; (2) independent of alkyl substrate the singlet and triplet C-H activation, barriers are nearly isoenergetic; and (3) highly unactivated alkyl substrates (e.g., methane and ethane) favor a HAT mechanism (from spin and charge analysis of the corresponding products) independent of the spin while for activated (2°, 3°, and benzyl) substrates both hydride and the HAT mechanism are competitive. Overall, we observe that the mechanism for C-H activation from the singlet biradical is sensitive to substituent effects, while the hydride mechanism is operative from the triplet biradical independent of the nature of the substrate.

That is, from a singlet biradical, the alkyl substrates capable of stabilizing positive charge (e.g., through inductive effects; secondary and tertiary) proceed via a hydride transfer step, leading to formation of a carbocationic F complex, while methyl and primary substrates proceed exclusively via the HAT mechanism.

2.5. Molecular Dynamics Simulations To Investigate the Nature of the N-H Bond Formation Step. To further explore the timing and formation of the N-H bond formation step in more detail, molecular dynamics simulations (MD) on TS_{D-F} were performed using Singleton's Progdyn program.¹⁹ To minimize the computational cost, a truncated system was studied in which the aryl and sulfonyl groups of the catalyst were replaced by an alkene and methyl, respectively (Scheme 8). MD simulations were performed in the gas phase using UB3LYP/6-31G(d) from the open-shell singlet and triplet transition states located using UM06-2X/6-31+G(d,p)-CPCM(dichloromethane) in Gaussian 16. As shown in Scheme 8 (bottom), the structural and energetic features (e.g., relative energetics between the singlet and triplet transition states) of the full system are preserved in the truncated system.

A typical trajectory involving N—H bond formation from the singlet biradical is shown in Scheme 9. In this trajectory, the hydride (N—H bond of <1.0 Å) is transferred within 12 fs from the tertiary carbon substrate to the nitrogen of the diaminium species. The trajectory continues for an additional 397 fs without any further bond formation or breaking events. These results show that hydride transfer (via singlet spin state) leads to the formation of a persistent (i.e., without rebound) carbocationic complex. Overall, 108 simulations were performed, and the results from analyzing these simulations show that most trajectories (84%) lead to the formation of the

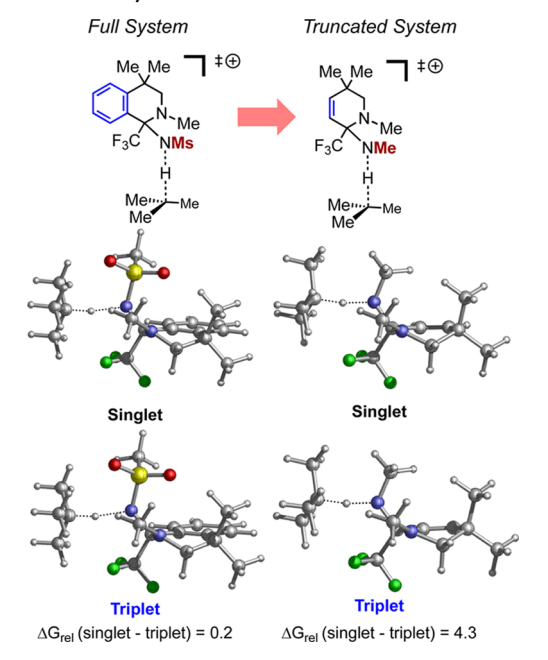
Scheme 7. Effect of Substrate (Methyl, Primary, Secondary, and Benzylic) and Spin State on Mechanism^a



"For the tertiary substrates, see Figures S9 and S10. Bond lengths are also given as Mulliken charge (black) and spin (red) of the central carbon atom of the substrate. Free energies (kcal/mol) are computed at the UB3LYP-D3/6-311+G(d,p)-SDD(I)-CPCM(DCM)//UM06-2X/6-31+G(d,p)-LANL2DZ(I)-CPCM(dichloromethane) level of theory (see Figure S21 in the Supporting Information for electrostatic potential maps).

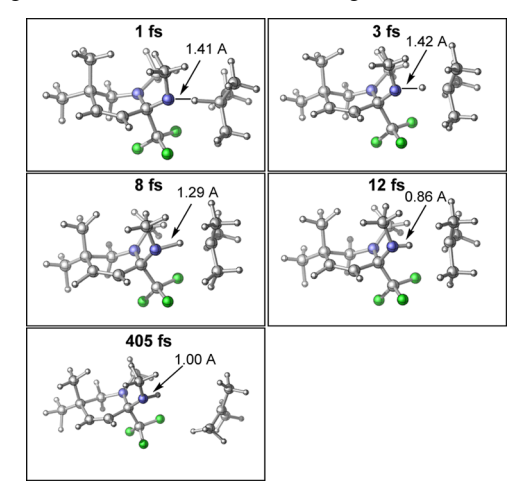
carbocationic complex F (Scheme 10). The reverse reaction leading to the open, singlet biradical D is also observed in 10%

Scheme 8. Singlet and Triplet Transition States for the Full and Truncated Systems a



"Free energies (kcal/mol) are computed at the UB3LYP-D3/6-311+G(d,p)-SDD(I)-CPCM(DCM)//UM06-2X/6-31+G(d,p)-LANL2DZ(I)-CPCM(dichloromethane) level of theory.

Scheme 9. Snapshots of a Typical Reactive Trajectory Propagated in the Gas Phase, Leading to Intermediate F^a

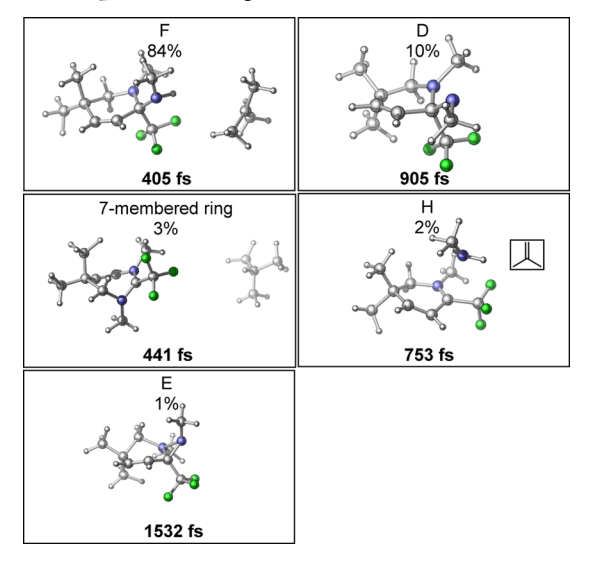


^aThe hydrogen is transferred in the first 12 fs of the trajectory.

of the trajectories, while only $\sim 1\%$ (after 1532 fs) of the trajectories lead to the much lower energy 3-membered diaziridinium E. These results suggest that a long-lived biradical species is responsible for C–H amination.

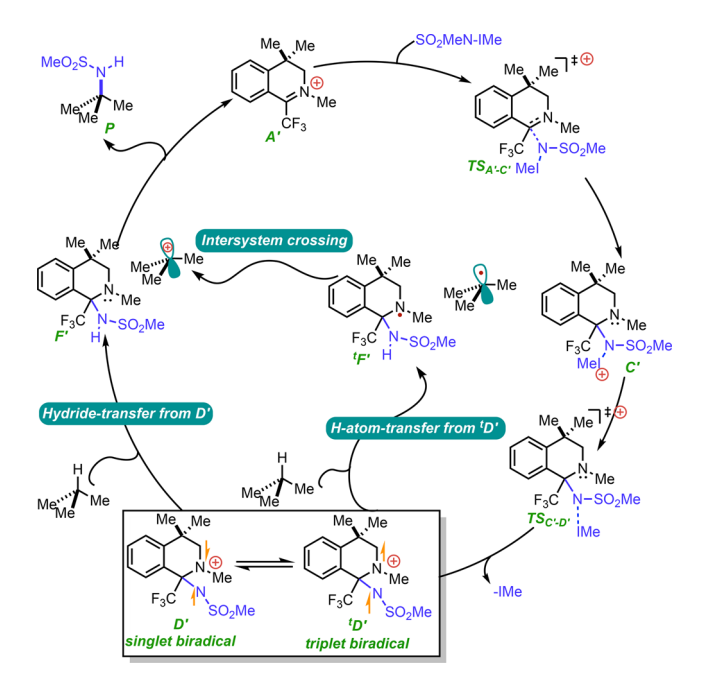
Consistent with this hypothesis, we also observed ringexpansion product (7-membered ring) in ~3% of the trajectories (after ~441 fs), similar to the decomposition products of diaziridiniums that have previously been observed experimentally (see Figure S22 in the Supporting Information for the potential energy surface including this side pathway). Notably, we previously published experimental results that support the notion that a tosyl or other sulfonyl groups lower the tendency of the organocatalyst to undergo ring expansion

Scheme 10. Summary of Results from 108 MD Simulations from the Open-Shell Singlet Transition State Located



relative to hydrogen,⁷ consistent with the calculations showing ring expansion as a minor pathway. We are currently exploring the effect of the tosyl group in the dynamics. Finally, we also observed ~2% of the simulations leading to intermediate H in which a second hydrogen from the tertiary carbocation is abstracted by the amine group, leading to 2-methyl propene, methyl amine, and regeneration of the iminium organocatalyst. Overall, these results support the mechanism shown in Scheme 11 and do not support a rapid rebound mechanism. However, in our calculations we do not consider explicit solvent molecules and counterions, which are likely to play a key role in preventing the escape of discrete carbocations to undergo side bimolecular reactions.

Scheme 11. Mechanism of Organocatalytic C-H Amination As Revealed by Quantum Mechanical and Quasi-classical Dynamic Calculations



2.6. Correlation of Computational to Experimental Results and Implications for Future Reaction Design.

The initial hypothesis guiding the design of iminium-catalyzed C-H amination was centered on the idea that a diaziridinium might be accessed from the reaction of a nitrene precursor and the catalyst. Furthermore, that diaziridinium, like its cousins in the dioxirane and oxaziridine families, might be expected to transfer a heteroatom (in this case nitrogen) in a C-H functionalization process. Indeed, our calculations predict the formation of the expected diaziridinium as an intermediate along the reaction coordinate leading to C-H amination. However, unexpectedly and in contrast to the well-studied dioxirane case, the open biradical forms D and D' are also calculated to exist as intermediates and are found to be the relevant oxidants engaged in C-H bond cleavage. This result, along with the calculated nature of the subsequent C-H activation steps for each intermediate, is consistent with experimental results and provides important insight for future reaction design.

Experimentally and under conditions slightly modified from the computational model (i.e., use of PhINTs or PhINTces as the nitrene precursor), successful C-H amination is limited to benzylic C-H bonds or other C-H bonds that are substantially weakened by conjugative or hyperconjugative effects (see examples in Schemes 1 and 2). Calculations suggest that, whereas hydride transfer and HAT transition states are isoenergetic for primary, secondary, and tertiary C-H bonds, benzylic hydride transfer begins to be favored (by 0.6 kcal/mol for toluene as shown in Scheme 6). Previously, when studying the effect of substitution of the tetralin aromatic ring on relative reaction rates, we observed a strong correlation with the Hammett constant σ_p with a ρ value of -2.5.⁷ This suggests an increase in positive charge at the benzylic carbon. These data could be taken as evidence that, for the reported experimental results, a hydride transfer pathway via the singlet biradical is favored. Our previous investigations also found a primary kinetic isotope effect of 2.5 for amination of isochroman in an intermolecular competition experiment. We computed the kinetic isotope effect (KIE) of the H transfer step for both the down and up conformers of the N-H bond formation transition state. The computed values of $k_{\rm H}/k_{\rm D}^{20}$ were 1.72 and 1.98 for the down and up conformers, respectively, in our truncated system. These computed KIE values are in accord with the experimental value ($k_{\rm H}/k_{\rm D} = 2.5$) for the isochroman molecule (see Figure S23 in the Supporting Information). The magnitude of this effect is also consistent with predicted KIE values for reactions involving hydride transfer.²¹ In addition, the observation of a primary KIE is consistent with the overall mechanism that we propose, which shows that for benzylic amination, the rate-determining step is formation of D and D', but an irreversible C-H bond cleavage occurs in a product-determining step following the ratedetermining step.

The calculated mechanism and reaction barriers offer several potentially productive directions for reaction design. First, it is notable that both the overall barriers and calculated transition state energies for the C–H functionalization step (<20 kcal/mol in all cases) are lower than what might be predicted for a reaction exhibiting a scope at room temperature limited to benzylic or highly activated alkane substrates. One possible explanation for this is that the generation of an *N*-tosyl analog of **D** might, for steric reasons, occur with a higher barrier, and that this analog might subsequently exhibit lower reactivity

than the calculated N-mesyl oxidant, given the proximity of the nitrogen protecting group to the substrate during the C-H functionalization step (Scheme 7). In this regard, reducing the steric bulk of the terminal oxidant is potentially of interest. Moreover, the lack of reactivity with otherwise unactivated tertiary C-H bonds is puzzling given that formation of D is calculated to be the rate-determining step, as in the benzylic case. Sterics might play a role here. However, we also observe that PhINTs and PhINTces are poorly soluble in the reaction mixture and dissolve slowly (and not always entirely) over the time period of the reaction. Therefore, an alternative hypothesis is that the poor solubility of the terminal oxidant severely limits the concentration of D and D' in the reaction mixture, leading to rates of product formation that are below an observable level. This might be addressed by the use of more soluble nitrene precursors. We are currently investigating the effect of these factors on reaction performance.

3. CONCLUSIONS

We explored the mechanism of iminium-catalyzed C-H amination through computational methods including quantum mechanical calculations and molecular dynamics simulations. Through our computational studies, we have proposed a mechanism by which this C-H amination occurs. The iminoiodinane is added to the iminium catalyst followed by removal of the iodomethane. The resulting singlet biradical species can then undergo N-H bond formation. Our computational studies show that both hydride transfer and HAT mechanisms for activated C-H bonds are operative, competitive, and energetically accessible. However, for unactivated C-H bonds/sites (e.g., 1°), a HAT mechanism is operative but large energetic barriers are observed. Furthermore, in agreement with quantum mechanical calculations, molecular dynamics simulations do not support a rapid rebound mechanism. Modulating the organocatalyst to control the mechanism of C-H amination (hydride vs HAT mechanism) by tuning the substituents of the biradical intermediate is underway. Further MD calculations to explore the effect of explicit solvent and counterions in the mechanism and modifications to reaction parameters suggested by the proposed mechanism are underway and will be reported in due course.

ASSOCIATED CONTENT

S Supporting Information

The Supporting Information is available free of charge at https://pubs.acs.org/doi/10.1021/acscatal.9b03588.

Computational details, energies, and coordinates for all structures (PDF)

AUTHOR INFORMATION

Corresponding Authors

*E-mail: hilinski@virginia.edu (M.K.H.).

*E-mail: ogs@umd.edu (O.G.).

ORCID ®

Madeline E. Rotella: 0000-0002-7973-2452 Michael K. Hilinski: 0000-0003-2861-7099 Osvaldo Gutierrez: 0000-0001-8151-7519

Notes

The authors declare no competing financial interest.

ACKNOWLEDGMENTS

O.G. is grateful for the financial support provided by NSF (CAREER, 1751568), and M.K.H. is grateful to the National Institutes of Health (R01 GM124092) for funding. O.G. is grateful to the University of Maryland College Park for startup funds and computational resources from UMD Deepthough2 and MARCC/BlueCrab HPC clusters and XSEDE (CHE 160082 and CHE160053).

REFERENCES

- (1) Vitaku, E.; Smith, D. T.; Njardarson, J. T. Analysis of the Structural Diversity, Substitution Patterns, and Frequency of Nitrogen Heterocycles Among U.S. FDA Approved Pharmaceuticals. *J. Med. Chem.* **2014**, *57*, 10257–10274.
- (2) Blakemore, D. C.; Castro, L.; Churcher, I.; Rees, D. C.; Thomas, A. W.; Wilson, D. M.; Wood, A. Organic Synthesis Provides Opportunities to Transform Drug Discovery. *Nat. Chem.* **2018**, *10*, 383–394
- (3) Park, Y.; Kim, Y.; Chang, S. Transition Metal-Catalyzed C-H Amination: Scope, Mechanism, and Applications. *Chem. Rev.* **2017**, *117*, 9247–9301.
- (4) For representative recent examples see: (a) Clark, J. R.; Feng, K.; Sookezian, A.; White, M. C. Manganese-Catalysed Benzylic C(sp³)-H Amination for Late-Stage Functionalization. Nat. Chem. 2018, 10, 583-591. (b) Chiappini, N. D.; Mack, J. B. C.; Du Bois, J. Intermolecular C(sp³)-H Amination of Complex Molecules. Angew. Chem., Int. Ed. 2018, 130, 5050-5053. (c) Prier, C. K.; Zhang, R. K.; Buller, A. R.; Brinkmann-Chen, S.; Arnold, F. H. Enantioselective, Intermolecular Benzylic C-H Amination Catalysed by an Engineered Iron-Haem Enzyme. Nat. Chem. 2017, 9, 629-634. (d) Dolan, N. S.; Scamp, R. J.; Yang, T.; Berry, J. F.; Schomaker, J. M. Catalyst-Controlled and Tunable, Chemoselective Silver-Catalyzed Intermolecular Nitrene Transfer: Experimental and Computational Studies. J. Am. Chem. Soc. 2016, 138, 14658-14667. (e) Bess, E. N.; DeLuca, R. J.; Tindall, D. J.; Oderinde, M. S.; Roizen, J. L.; Du Bois, J.; Sigman, M. S. Analyzing Site Selectivity in Rh₂(esp)₂-Catalyzed Intermolecular C-H Amination Reactions. J. Am. Chem. Soc. 2014, 136, 5783-5789. (f) Roizen, J. L.; Zalatan, D. N.; Du Bois, J. Selective Intermolecular Amination of C-H Bonds at Tertiary Carbon Centers. Angew. Chem., Int. Ed. 2013, 52, 11343-11346.
- (5) Hazelard, D.; Nocquet, P.-A.; Compain, P. Catalytic C-H Amination at Its Limits: Challenges and Solutions. *Org. Chem. Front.* **2017**, *4*, 2500–2521.
- (6) Johnson, S. L.; Combee, L. A.; Hilinski, M. K. Organocatalytic Atom-Transfer $C(sp^3)$ –H Oxidation. *Synlett* **2018**, *29*, 2331–2336.
- (7) Combee, L. A.; Raya, B.; Wang, D.; Hilinski, M. K. Organocatalytic Nitrenoid Transfer: Metal-Free Selective Intermolecular C(sp³)–H Amination Catalyzed by an Iminium Salt. *Chem. Sci.* **2018**, *9*, 935–939.
- (8) Johnson, S. L.; Hilinski, M. K. Organocatalytic Olefin Aziridination via Iminium-Catalyzed Nitrene Transfer: Scope, Limitations, and Mechanistic Insight. J. Org. Chem. 2019, 84, 8589–8595
- (9) Allen, J. M.; Lambert, T. H. Synthesis and Characterization of a Diaziridinium Ion. Conversion of 3,4-Dihydroisoquinolines to 4,5-Dihydro-3H-Benzo [2,3] Diazepines via a Formal N-Insertion Process. *Tetrahedron* **2014**, *70*, 4111–4117.
- (10) (a) Lusinchi, X.; Hanquet, G. Oxygen transfer reactions from an Oxaziridinium tetrafluoroborate salt to Olefins. *Tetrahedron* 1997, 53, 13727–13738. (b) Hanquet, G.; Lusinchi, X.; Milliet, P. Transfert d'oxygene sur la double liaison ethylenique a partir d'un sel d'oxaziridinium. *Tetrahedron Lett.* 1988, 29, 3941–3944. (c) Bohé, L.; Hanquet, G.; Lusinchi, M.; Lusinchi, X. The stereospecific synthesis of a new chiral oxaziridinium salt. *Tetrahedron Lett.* 1993, 34, 7271–7274. Bohé, L.; Lusinchi, M.; Lusinchi, X. Oxygen atom transfer from a chiral oxaziridinium salt. Asymmetric epoxidation of unfunctionalized olefins. *Tetrahedron* 1999, 55, 141–154. (d) Aggarwal, V. K.; Wang, M. F. Catalytic asymmetric synthesis of epoxides

mediated by chiral iminium salts. *Chem. Commun.* **1996**, 191–192. (e) Armstrong, A.; Ahmed, G.; Garnett, I.; Goacolou, K. Pyrrolidine-Derived Iminium Salts as Catalysts for Alkene Epoxidation by Oxone. *Synlett* **1997**, 1075–1076. (f) Bulman Page, P. C.; Rassias, G. A.; Bethell, D.; Schilling, M. B. A New System for Catalytic Asymmetric Epoxidation Using Iminium Salt Catalysts. *J. Org. Chem.* **1998**, 63, 2774–2777.

- (11) (a) Curci, R.; Dinoi, A.; Fusco, C.; Lillo, M. A. On the Triggering of Free Radical Reactivity of Dimethyldioxirane. *Tetrahedron Lett.* **1996**, 37, 249–252. (b) Murray, R. W. Chemistry of dioxiranes. 12. Dioxiranes. *Chem. Rev.* **1989**, 89, 1187–1201.
- (12) We attempted to locate this concerted transition state A-TS but all efforts, including using restricted and unrestricted DFT, led to the stepwise pathway. In addition, we froze the geometry to locate the concerted transition state but releasing constraints led to the stepwise pathway as well.
- (13) Gassman, P. G. Nitrenium Ions. Acc. Chem. Res. 2002, 3, 26–33.
- (14) Srivastava, S.; Kercher, M.; Falvey, D. E. On the solution chemistry of parent nitrenium ion $\mathrm{NH_2}^+$: The role of the singlet and triplet states in its reactions with water, methanol, and hydrocarbons. *J. Org. Chem.* **1999**, *64*, 5853–5857.
- (15) (a) Al-Bataineh, N.; Houk, K. N.; Brewer, M.; Hong, X. (2+1)-Cycloaddition Reactions Give Further Evidence of the Nitrenium-like Character of 1-Aza-2-azoniaallene Salts. *J. Org. Chem.* **2017**, 82, 4001–4005. (b) Cleary, S. E.; Li, X.; Yang, L.-C.; Houk, K. N.; Hong, X.; Brewer, M. Reactivity Profiles of Diazo Amides, Esters, and Ketones in Transition-Metal-Free C—H Insertion Reactions. *J. Am. Chem. Soc.* **2019**, 141, 3558–3565. (c) Zhu, C.; Liang, Y.; Hong, X.; Sun, H.; Sun, W.-Y.; Houk, K. N.; Shi, Z. Iodoarene-Catalyzed Stereospecific Intramolecular sp³ C—H Amination: Reaction Development and Mechanistic Insights. *J. Am. Chem. Soc.* **2015**, 137, 7564–7567.
- (16) We are aware the issues that exist with single reference formalism in modeling these nitrenium species. However, for this study, we did not turn to multireference calculations (e.g., CASPT2/ CASSCF) due to the prohibitively high computational cost associated with these types of calculations in such a complex mechanism. Furthermore, studies by Winter in which both DFT and CASPT2 were used to model open-shell species and the trends predicted by DFT methods agree with multireference methods although the calculated singlet-triplet energy gap differs by 2-4 kcal/mol depending on the method from experiment. For further discussion of this topic, refer to the following. (a) Winter, A. H.; Falvey, D. E.; Cramer, C. J.; Gherman, B. F. Benzylic Cations with Triplet Ground States: Computational Studies of Aryl Carbenium Ions, Silylenium Ions, Nitrenium Ions, and Oxenium Ions Substituted with Meta π Donors. J. Am. Chem. Soc. 2007, 129, 10113-10119. (b) Albright, T. R.; Winter, A. H. A Fine Line Separates Carbocations from Diradical Ions in Donor-Unconjugated Cations. J. Am. Chem. Soc. 2015, 137, 3402-3410. (c) Cramer, C. J.; Dulles, F. J.; Falvey, D. E. Ab Initio Characterization of Phenylnitrenium and Phenylcarbene: Remarkably Different Properties for Isoelectronic Species. J. Am. Chem. Soc. 1994, 116, 9787-9788. (d) Cramer, C. J.; Truhlar, D. G.; Falvey, D. E. Singlet-Triplet Splittings and 1,2-Hydrogen Shift Barriers for Methylphenylborenide, Methylphenylcarbene, and Methylphenylnitrenium in the Gas Phase and Solution. What a Difference a Charge Makes. J. Am. Chem. Soc. 1997, 119, 12338-12342. (e) Geise, C. M.; Hadad, C. M. Computational Study of the Electronic Structure of Substituted Phenylcarbene in the Gas Phase. J. Org. Chem. 2000, 65, 8348-8356. (f) McIlroy, S.; Cramer, C. J.; Falvey, D. E. Singlet-Triplet Energy Gaps in Highly Stabilized Nitrenium Ions: Experimental and Theoretical Study of 1,3-Dimethylbenzotriazolium Ion. Org. Lett. 2000, 2, 2451-2454. (g) Trindle, C. DFT Studies of Biarylcarbenes and the Carbene-Biradical Continuum. Org. Chem. 2003, 68, 9669-9677.
- (17) Kuzmanich, G.; Spänig, F.; Tsai, C.-K.; Um, J. M.; Hoekstra, R. M.; Houk, K. N.; Guldi, D. M.; Garcia-Garibay, M. A. Oxyallyl Exposed: An Open-Shell Singlet with Picosecond Lifetimes in

Solution but Persistent in Crystals of a Cyclobutanedione Precursor. *J. Am. Chem. Soc.* **2011**, *133*, 2342–2345.

- (18) Hamlin, T. A.; Kelly, C. B.; Ovian, J. M.; Wiles, R. J.; Tilley, L. J.; Leadbeater, N. E. Toward a Unified Mechanism for Oxoammonium Salt-Mediated Oxidation Reactions: A Theoretical and Experimental Study Using a Hydride Transfer Model. *J. Org. Chem.* **2015**, *80*, 8150—8167.
- (19) Singleton, D. A.; Wang, Z. Isotope Effects and the Nature of Enantioselectivity in the Shi Epoxidation. The Importance of Asynchronicity. J. Am. Chem. Soc. 2005, 127, 6679–6685.
- (20) Anderson, T. L.; Kwan, E. E. *PyQuiver* 2016, www.github.com/ekwan/PyQuiver.
- (21) Shen, G.-B.; Xia, K.; Li, X.-T.; Li, J.-L.; Fu, Y.-H.; Yuan, L.; Zhu, X.-Q. Predicition of Kinetic Isotope Effects for Various Hydride Transfer Reactions Using a New Kinetic Model. *J. Phys. Chem. A* **2016**, *120*, 1779–1799.